Journal of materials and Environmental Sciences
ISSN : 2028-2508

JMES, 2017 Volume 8, Issue 2, Page 485-493

http://www.jmaterenvironsci.com/

Effect of annealing treatment on Co_3O_4 thin films properties prepared by spray pyrolysis

A. Louardi[1,2*], A. Rmili[2], T. Chtouki[2], B. Elidrissi[2], H. Erguig[2], A. El Bachiri[3], K. Ammous[4] and H. Mejbri[4].

[1] *Laboratoire de Physique de la Matière Condensée (LPMC), Département de physique, Faculté des sciences, Université Chouaib-Doukkali, El Jadida, Morocco*

[2] *Laboratoire d'Ingénieries des Systèmes Electriques et des Télécommunications, Ecole Nationale des Sciences Appliquées de Kénitra (ENSAK), Morocco*

[3] *Laboratoire Bio-Géosciences et Ingénierie des Matériaux (LBGIM), Ecole normale supérieure, Université Hassan II, BP 50069 Casablanca, Morocco*

[4] *Groupe d'Electronique de Puissance (PEG), Ecole Nationale d'Ingénieurs de Sfax (ENIS),Tunisia*

Received 05 Oct 2015,
Revised 21 Oct 2016,
Accepted 25 Oct 2016

Keywords
- ✓ Cobalt oxide,
- ✓ Thin films,
- ✓ Annealing treatment,
- ✓ Electrical properties.

louardiphysique@gmail.com;
Tel: +212676612157

Abstract

Cobalt oxide (Co_3O_4) thin films were deposited on amorphous glass substrates by spray pyrolysis method. The as deposited films were annealed at temperature ranging from 300 to 500°C. The characterization of samples was carried out by X-Ray diffraction, scanning electron microscopy, UV-VIS spectroscopy and electrical conductivity. Results showed that all the films were polycrystalline spinel type cubic structure. The preferred orientation of the crystallites changed from (111) for the as deposited films to (311) after annealing treatments. The scanning electron microscopy (SEM) images showed nanocrystalline grains size with porous structure. The optical transmittance and the electrical conductivity increased slightly with increasing the annealing temperature, indicating an improvement of the crystallinity of the films. The temperature dependence of the dc conductivity gave evidence of a transport mechanism based on the three dimensional Mott's variable-range hopping.

1. Introduction

Cobalt oxide (Co_3O_4) thin films have attracted substantial research effort in recent years because their potential application in various technological areas. They can be used as high temperature solar selective absorbers [1], anodic electrochromic materials in smart window devices [2] and negative electrodes in lithium-ion batteries [3]. Cobalt oxide exists in three different crystalline forms, namely CoO, Co_2O_3 and Co_3O_4 [4]; but the latter stoichiometry is reported for the electrochemical applications because of its spinel structure that contains vacancy and its chemical stability. Co_3O_4 thin films were prepared by employing different techniques such as RF magnetron sputtering [5], atomic layer deposition [6], chemical vapor deposition [7], sol–gel process [8], co-precipitation method [9], pulsed laser deposition [10] chemical bath deposition [11] and spray pyrolysis [12]. Among these deposition techniques, spray pyrolysis has several advantages: its low cost, flexibility, convenience for large deposition area and capability for preparing nanostructure thin films. This technique has been used successfully in our laboratory to fabricate a variety of porous materials for electrochromic devices such as WO_3 [13], Fe_2O_3 [14], CeO_2 [15] and Co_3O_4 [16]. It was shown that the porous structure is highly desired to improve the electrochromic performances of Co_3O_4 thin films since it can facilitate the intercalation/desintercallation of small ions such as H^+, Li^+, Na^+. Thus, controlling the morphology of Co_3O_4 thin films is very important.

In the present work, we have studied the effect of annealing temperature on the structural, morphological, optical and electrical properties of the Co_3O_4 thin films elaborated by a simplified spray pyrolysis technique using perfume atomizer. It was shown that the structural, optical and electrical properties of Co_3O_4 films were improved by increasing the annealing temperature.

2. Materials and methods

2.1. Preparation of the films

Cobalt oxide thin films were prepared from solution of hydrated cobalt chloride ($CoCl_2$, $6H_2O$) dissolved in 50 ml of deionized water, stirred thoroughly using a magnetic stirrer for 20 min and then sprayed manually in fine droplets using a perfume atomizer on the pre-heated glass substrate kept at different temperatures. Before the deposition process, the glass substrates were degreased with organic solvent, rinsed with deionized water and dried in air.

2.2. Characterization

The as deposited films were black in color and found to be uniform, pinholes free and strongly adherent to the glass substrates. Their thickness was calculated by using gravimetric method assuming the samples were approximately uniform as that of bulk having density of 8.6 $g.cm^{-3}$. The thickness of Co_3O_4 thin films was found to vary from 450 to 500 nm with an accuracy of 10%. The structure, crystallinity and phase of the Co_3O_4 thin films were determined by the X-ray diffraction (XRD) analysis, using Cu Kα radiation with 2θ ranging from 15° to 80°. The surface morphology of the films was characterized by scanning electron microscopy (SEM). In order to determine the band gap energy of Co_3O_4 in thin film form, the optical transmission studies were carried out in the wavelength range of 300–1500 nm, using a SHIMADZU 3101 PC UV-VIS-NIR spectrophotometer. Measurements of electric resistivity were carried out at dark and at room temperature. The variation of electrical resistivity with temperature was measured with the four-probe technique using keithley 2400.

3. Results and discussion

3.1. Crystal structure determination

Fig.1(a)-(d) shows the XRD patterns of Co_3O_4 thin films as deposited and annealed at different temperatures of 300, 400 and 500°C. All the films, as deposited and annealed, show multiple diffraction peaks at 2θ = 18.9°, 31.3°, 36.9°, 44.9°, 59.5° and 79.02°, indicating their polycrystalline nature. The inter-planar spacing values corresponding to the (111), (220), (311), (222), (400), (511), (440), and (622) diffraction planes compared with the standard values of Co_3O_4 [17]. A matching of the calculated d_{hkl} values and the standard ones confirms that the as deposited and annealed films are crystallized in the spinel type cubic structure of Co_3O_4 (Fd3m space group). Before annealing, the films have a preferential orientation along the (111) direction. After annealing, the preferred orientation changes from (111) to (311) direction. This change of preferred orientation of Co_3O_4 thin films after annealing might be due to the annealing treatment process. However, Chougule et al. [18] and Patil et al. [19] who prepared Co_3O_4 thin films by sol-gel and by spin coating technique respectively have found a random orientation for their films after annealing between 400 and 700°C. Moreover, the Co_3O_4 thin films were formed in a single-phase, suggesting that Co_3O_4 is more stable. M. Hamdani et al. [20] have also obtained a single-phase for Co_3O_4 films prepared by spray pyrolysis after annealing temperature, while Avila et al. [21] have observed the appearance of some XRD peak reflections corresponding to CoO and Co_2O_3.

It is also observed in Fig.1 that the XRD peaks became sharper by increasing the temperature of annealing treatment, which indicates that the crystallinity of the films is improved. The preferred orientation of the Co_3O_4 thin films is evaluated by the texture coefficient (T_C) from the X-ray data using the well-known formula:

$$T_C(hkl) = \frac{I(hkl)/I_0(hkl)}{\frac{1}{N}\sum_{hkl} I(hkl)/I_0(hkl)} \qquad (1)$$

Where T_C(hkl) the texture coefficient of the hkl planes, *I(hkl)* is the measured or normalized intensity, I_0 the corresponding standard intensity given in JCPDS data, and N the number of reflections. Fig.2 presents T_C(hkl) values calculated from the above equation (1) for the reflections (111) and (311) of as deposited and annealed Co_3O_4 thin films. It is observed that with all the annealing temperatures, the (311) diffraction peak has the highest T_C value. The lattice parameter 'a' of the unit cell is calculated from the peak positions using the formula of cubic system:

$$d_{hkl} = \frac{a}{\sqrt{(h^2 + k^2 + l^2)}} \qquad (2)$$

The value is found to be in the range 8,087-8.099 Å, which is close to the one given by JCPDS 42-1467 (a = 8.084 Å) [22]. The average crystallite size (D_{hkl}) of the Co_3O_4 thin films is estimated from the X-ray diffraction patterns using the Scherrer formula [23]:

$$D_{hkl} = 0.9 \frac{\lambda}{\beta_{hkl} \cos(\theta_{hkl})} \quad (3)$$

Where λ is the wavelength of incident radiation (λ = 1.544 Å), β_{hkl} is the full-width at half maximum (FWHM) of the preferential orientation diffraction peak and θ_{hkl} is the Bragg diffraction angle. The calculated values are reported in Table 1. As it can be seen, the crystallite size increases from 40 to 48 nm with increasing the annealing temperature from 300 to 500°C. This indicates that the cristallinity of the Co_3O_4 thin films is improved by increasing annealing temperature as it is found by XRD patterns. This result is in good agreement with that found by Chougule et al. [18] and Patil et al. [19] for annealed Co_3O_4 thin films prepared by sol-gel and spin coating techniques, respectively.

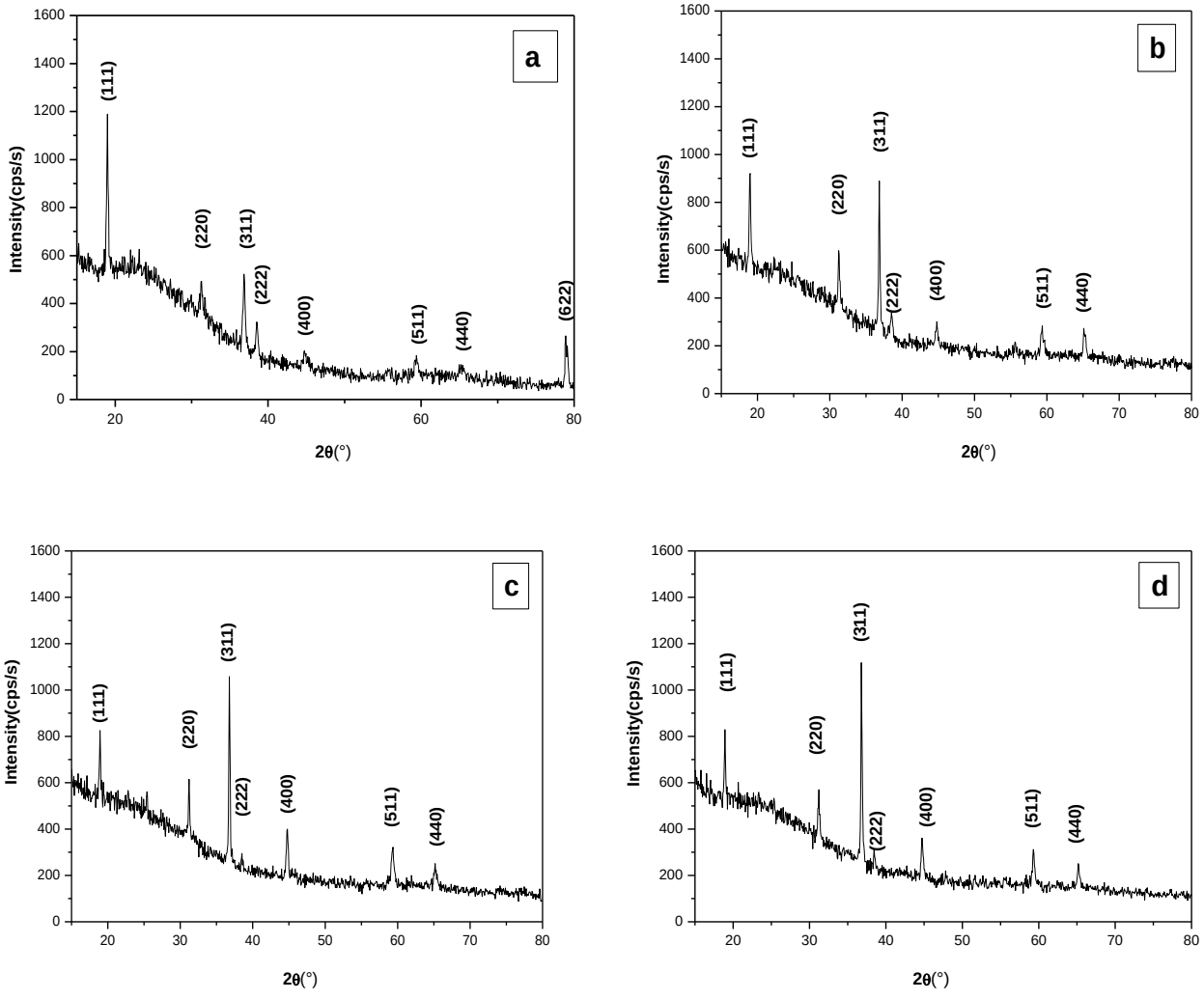

Figure 1: X-ray diffraction patterns of Co_3O_4 thin films: (a) as deposited, (b) annealed at 300°C, (c) annealed at 400°C, (d) annealed at 500°C.

Table 1: Average crystallite size of the Co_3O_4 thin films annealed at different temperatures.

annealing temperature	0	300°C	400°C	500°C
Average crystallite size (nm)	40	44	45	48

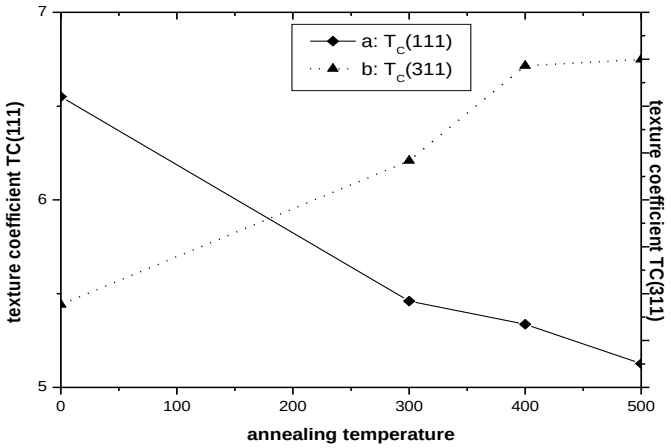

Figure 2: Variation of T_C(hkl) values with annealing temperature: (a) T_C(111), (b) T_C(311).

3.2. Surface morphology

The influence of annealing temperature on the surface morphology of the spray deposited Co_3O_4 thin films is studied by scanning electron microscopy technique. Fig. 3(a)–(d) shows the SEM images of as deposited and annealed Co_3O_4 thin films at 300 , 400 and 500°C at low magnification (× 20.000), It is clearly seen that the films have a heterogeneous surfaces with nanocrystalline grains and porous structure. The porous structure is highly desired to improve the electrochromic and catalytic performances of Co_3O_4 films. This porosity may be due to the evaporation of water molecular during the growing process and the annealing treatment.

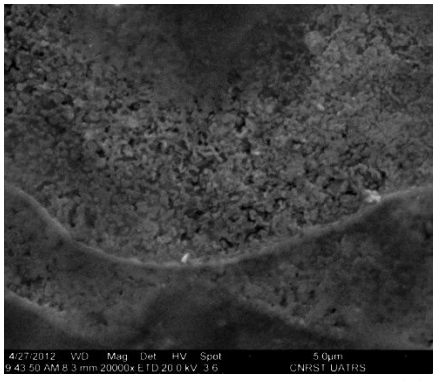

(a) (x 20.000)

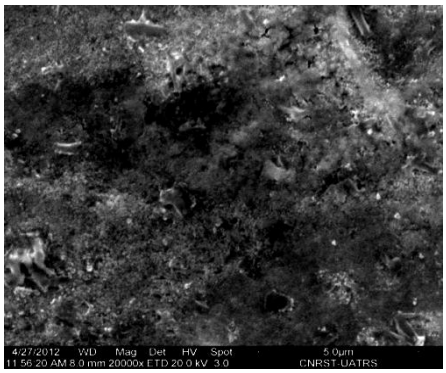

(b) (x 20.000)

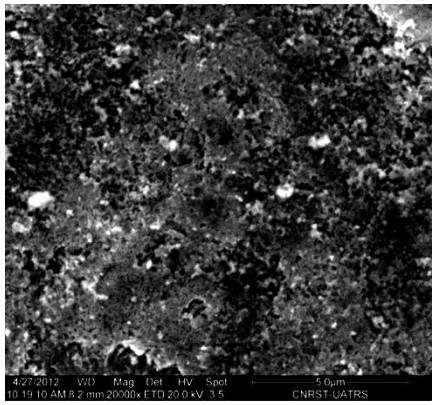

(c) (x 20.000)

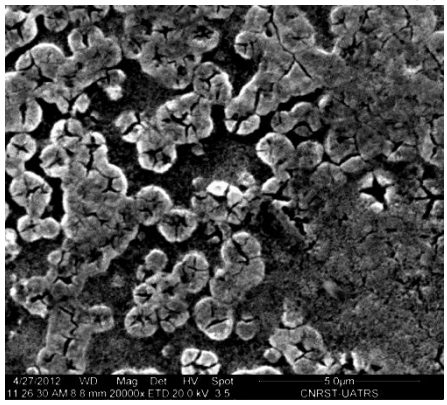

(d) (x 20.000)

Figure 3: SEM images of Co_3O_4 thin films (magnification 20.000×): (a) as deposited, (b) annealed at 300°C, (c) annealed at 400°C, (d) annealed at 500°C.

3.3. Optical properties

The optical properties such as the optical transmittance, absorption coefficient and band gap energy of Co_3O_4 thin films were determined from studying the variation of the optical transmission with wavelength (λ) in the range of 300 –1500 nm. Fig.4 shows plots of optical transmission of the as deposited and annealed Co_3O_4 thin films at different temperatures: (a) as deposited, (b) annealed at 300°C, (c) annealed at 400°C, (d) annealed at 500°C. It can be seen that the optical transparency improves with the increase of annealing temperature. This increase in transmittance can be explained by a relatively better crystallinity of the annealed films. Fig. 4 shows also two sharp absorption edges in the visible region. This indicates that the absorption band gap transitions in the Co_3O_4 thin films are direct. From the solid band theory, the relationship between the absorption coefficient α and the energy of the incident light hυ near the absorption edge of semiconductors is given by the Tauc's relation:

$$(\alpha h\nu) = A(h\nu - Eg)^n \quad (4)$$

where *A* is a constant, *Eg* the band gap energy and *n* a constant equal to 0.5, 2, 1.5 and 3 for allowed direct, allowed indirect, forbidden direct and forbidden indirect transitions, respectively. Fig. 5(a)-(d) shows the plots of $(h\upsilon)^2$ versus (hυ) for Co_3O_4 thin films as deposited (a) and after annealing treatment (b-d) at different temperatures. Two straight line portions have been observed, indicating the existence of two direct band gap values of Co_3O_4 which are in good agreement with the literature [24]. The band gap (Eg) of those films is in the range of 1.48–1.50 eV for lower energy side region and 2.07–2.18 eV for higher energy side region, which is consistent with the reported Co_3O_4 band structure [25–26]. It can also be seen that the Eg value increases slightly with increasing the annealing temperature. This suggests that the absorption edges shift to the higher energy as a consequence of the thermal annealing. The increase in optical band gaps indicates that the temperature affects the optical band gaps by changing the atomic distances of Co_3O_4 thin film, which leads to a decrease of the Urbach energy.

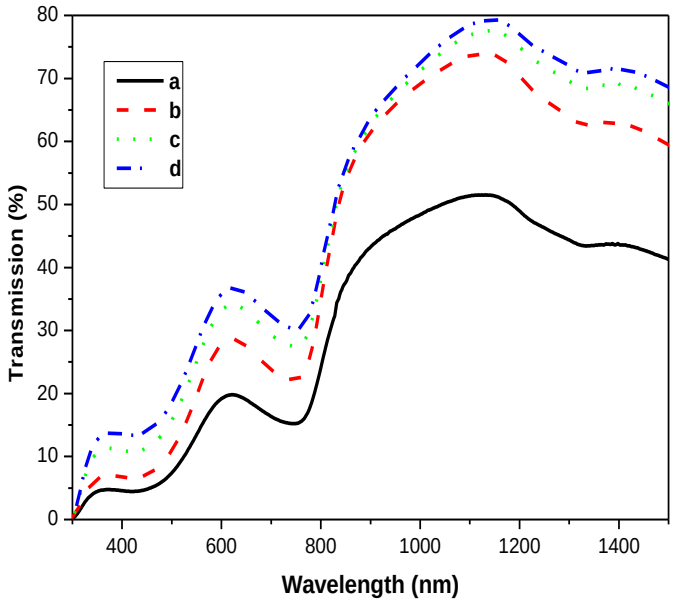

Figure 4: Plots of optical transmission of the Co_3O_4 thin films: (a) as deposited at 350°C, (b) annealed at 300°C, (c) annealed at 400°C, (d) annealed at 500°C.

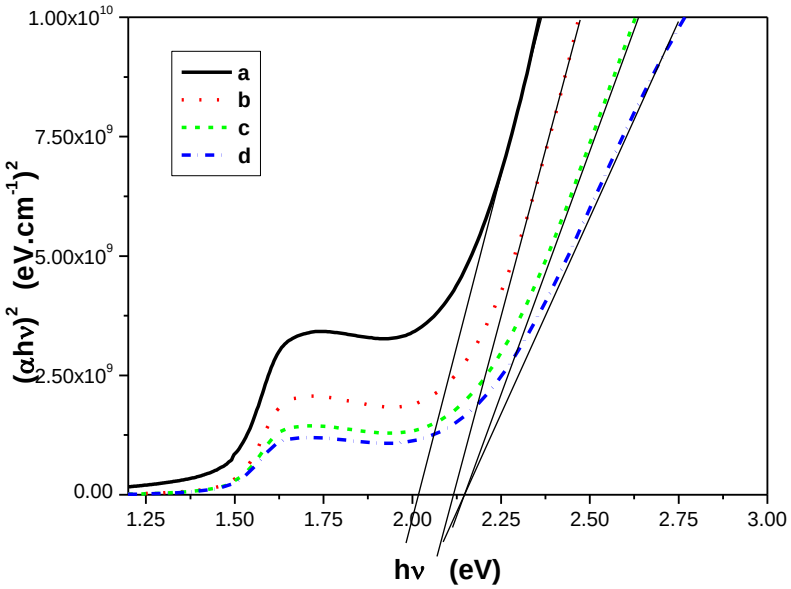

Figure 5: Plots of $(h\upsilon)^2$ versus $(h\upsilon)$ for Co_3O_4 thin films: (a) as deposited, (b) annealed at 300°C, (c) annealed at 400°C, (d) annealed at 500°C.

3.4. Electrical properties

The dark electrical conductivity at room temperature of the sprayed thin oxide Co_3O_4 films deposited onto non conductive substrate is found to be 1.5 x 10^{-4} (Ω^{-1}.cm^{-1}), and it increases with the increasing the annealing temperature (300-500°C) from 1.5 x 10^{-4} to 7.5 x 10^{-4} (Ω^{-1}.cm^{-1}) as it can be shown in Fig.6. In fact, annealing treatment provides sufficient thermal energy to the crystal which facilitates the electron delocalization through the elimination of a large number of defects.

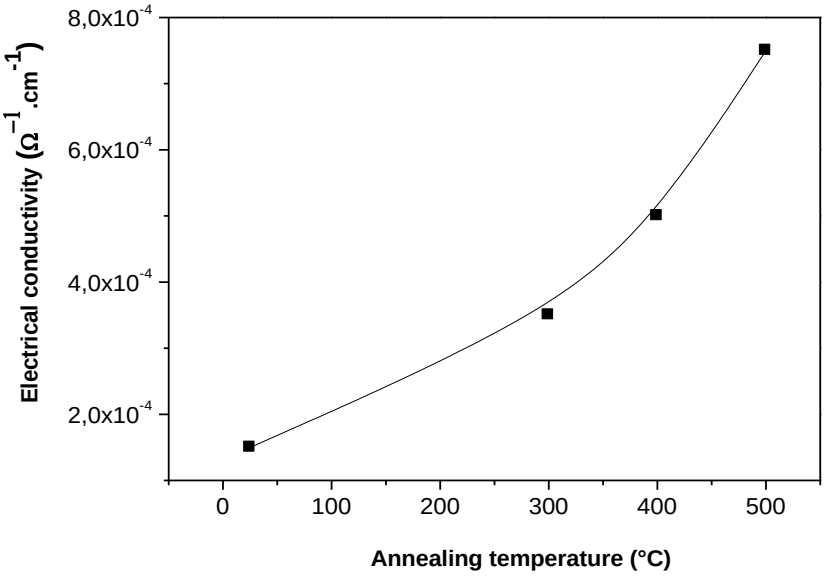

Figure 6: Variation of dark electrical conductivity at room temperature of the sprayed Co_3O_4 thin films deposited onto non-conductive substrate versus annealing temperature.

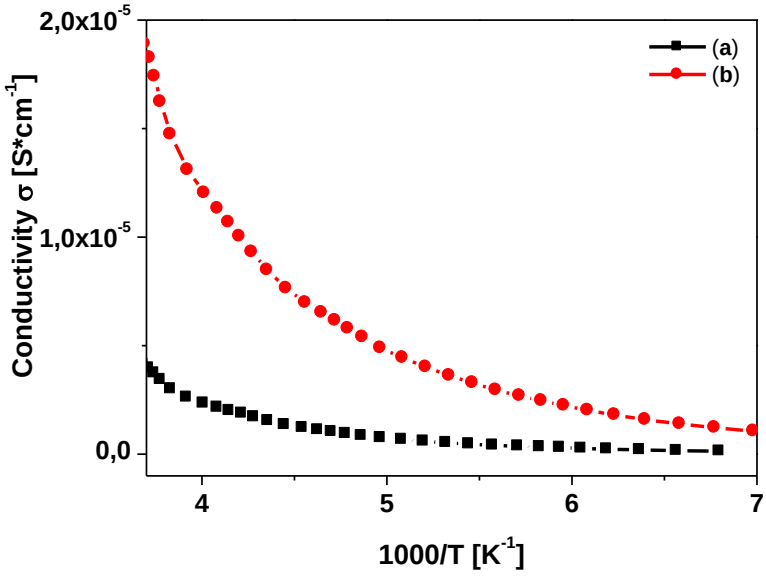

Figure 7: Variation of the electrical conductivity as function of temperature of Co_3O_4 thin films, (a) as deposited and (b) annealed at 500°C.

The four-probe technique was employed for measurement of variation of dark electrical conductivity of Co_3O_4 thin films with annealing temperature. Fig.7 displays the variation of electrical conductivity with reciprocal temperature (1000/T) of as deposited (a) and annealed at 500°C (b) cobalt oxide thin films. As it is shown, the electrical conductivity increases with the increase of temperature indicating the semiconductor nature of our thin films. We represented the variation of log σ with reciprocal temperature (1000/T) and we represented also the fit according of Arrhenius model (Equation 5).

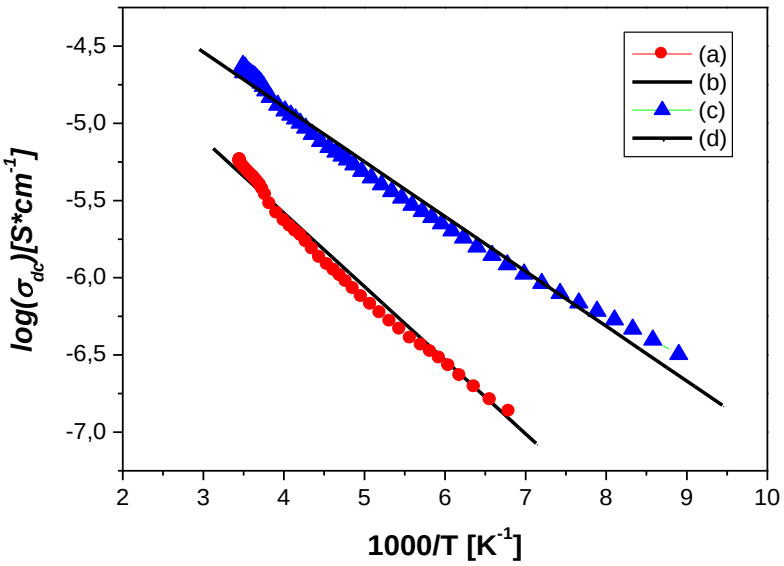

Figure 8: Log (σ) versus 1000/T of as deposited (a) and annealed at 500°C (c) thin films. The solid lines represent the fitting according to the Arrhenius model: (b) as deposited and (d) annealed at 500°C.

It is further observed that the conductivity σ cannot be fitted by the thermal excitation model given as:

$$\sigma(T) = \sigma_o \exp\left(\frac{w_a}{k * T}\right) \quad (5)$$

where, σ is the conductivity at temperature T, σ_0 is a constant, k is the Boltzmann constant, T is the absolute temperature and w_a is the activation energy.

We excluded the simple Arrhenius thermal excitation mechanism for the increased conductivity as temperature increases. Then we considered the hopping conduction models to fit the observed electrical properties. As proposed by Mott and co-workers [33, 34], a typical hopping mechanism, called variable range hopping (VRH), which takes place at low temperatures, is generally accepted for some semiconductor materials. The relationship between σ and T for the so-called (VRH) mechanism can be expressed by the following equation [33, 34]:

$$\sigma_{VRH}(T) = \sigma_o \exp\left(-\left[\frac{T_0}{T}\right]^{\frac{1}{4}}\right) \quad (6)$$

Where T_0 is the VRH characteristic temperature associated with the density of localized states at the Fermi energy N(EF). Fig. 8: depicts the VRH model for as deposited and annealed thin films from 54 K to 314 K. Since there is a good fit as indicated by solid lines of the experimental data according to Equation (6), the hopping conduction may be valid to explain the mechanism of carrier charge transport in Co_3O_4 of the present work.

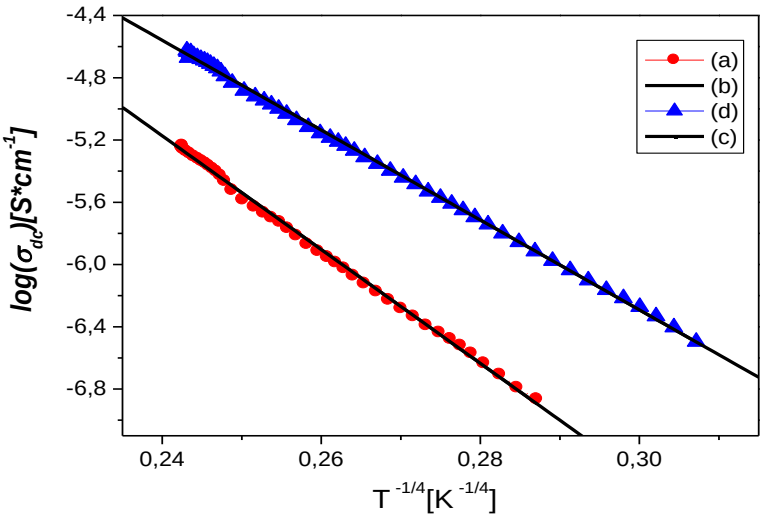

Figure 9: Log (σ) versus $T^{-1/4}$ of (a) as deposited and (c) annealed at 500°C of Co_3O_4 thin films. The solid lines represent the fitting according to the Mott model: (b) as deposited and (d) annealed at 500°C.

Conclusions

Nanocrystalline Cobalt oxide (Co_3O_4) thin films were deposited on amorphous glass substrate by spray pyrolysis method. The as prepared films were annealed at different temperatures (300 to 500°C). The X-Ray diffraction results showed that all the films were polycrystalline spinel type cubic structure. The preferred orientation of the crystallites of these films changed from (111) for the as deposited films to (311) after annealing treatments. The average crystallite size increased from 40 to 48 nm with the increasing annealing temperature from 300 to 500◦C. this indicated that the structural quality of Co_3O_4 films was improved by increasing the annealing temperature. The scanning electron microscopy (SEM) showed heterogeneous surfaces with grains and porous structure. The transmittance and the electrical conductivity were increased slightly with the increase of the annealing temperature, indicating an improvement of the optical and electrical properties of these thin films. An analysis of electrical properties, using the dc conductivity, showed that hopping of charges carriers between localized states was the dominant conduction mechanism.

Acknowledgements-The authors wish to express their gratitude to Professor A. Outzourhit (Laboratoire des couches minces, Faculté des Sciences de Marrakech-Semlalia) for his valuable help for optical measurements.

References

1. Barrera E., Huerta L., Muhl S., Avila A., *Solar Energy Mat. Sol. Cells* 88 (2005) 179.
2. Xia X.H., Tu J.P., Zhang J., Huang X.H., Wang X.L., Zhang W.K., Huang H., *Elec. Com.*10 (2008) 1815.
3. Shaju K.M., Jiao F., Debart A., Bruce P.G., *Physical Chem. Chem. Phy.* 9 (2007) 1837.
4. Kandalkar S.G., Lokande C.D., Mane R.S., Hun S.H., *Appl. Surf. Sci.* 253 (2007) 3952.
5. Liao C.L., Lee Y.H., Chang S.T., Fuang K.Z., *J. Pow. Sour.* 158 (2006) 1379.
6. Klepper K.B., Nilson O., Fjellvag H., *J. Cryst. Grow.* 307 (2006) 457.
7. Bahlawane N., Rivera E.F., Honghaus K.K., Brechling A., Kleinberg U., *Appl. Cat. B: Env.*53 (2004) 245.
8. Svegl F., Orel B., Svegl I.G., Kaucic V., *Electr. Acta* 45 (2000) 4359.
9. Pal J., Chauhan P., *Mat. Charact.* 61 (2010) 575.
10. Chou S.-L., Wang J.Z., Liu H.K., Dou S.H., *J. Pow. Sour.* 182 (2008) 359.
11. Fu Z.W., Wang Y., Zhang Y., Qin Q.Z., *Sol. St. Ionics* 170 (2004) 105.
12. Kadam L.D., Pawar S.H., Patil P.S., *Mat. Chem. Phy.* 68 (2001) 280.
13. Regragui M., Addou M., Outzourhit A., Bernede J.C., Elidrissi B., Benseddik E., Kachouane A., *Thin Sol. Fil.* 358 (2000) 40.
14. Dghoughi L., Elidrissi B., Addou M., Bernede J.C., Regragui M., Alaoui Lamrani M., Erguig H., *Appl. Surf. Sci.* 253 (2006) 1823.
15. Elidrissi B., Addou M., Regragui M., Monty C., Bougrine A., Kachouane A., *Thin Sol. Fil.* 379 (2000) 23.
16. Louardi A., Rmili A., Ouachtari F., Bouaoud A., Elidrissi B., Erguig H., *J. Alloys Comp.* 509 (2011) 9183.
17. Standard JCPDS Data Card, JCPDS 42-1467.
18. Chougule M.A., Pawar S.G., Godse P.R., Sakhare R.D., Shashwati Sen., Patil V.B., *J. Mat. Sci. Mat. in Elec.* 23 (2012) 772.
19. Patil V., Pawar S., Chougule M., Raut B., Mulik R., Sen S., *Sens. Trans.*128 (2011) 1726.
20. Hamdani M., Pereira M.I.S., Douch J., Ait Addi A., Berghoute Y., Mendonça M.H., *Electr. Acta* 49 (2004) 1555.
21. Avila A. G., Barrera E. C., Huerta L. A., Muhl S., *Solar Ener. Mat. Sol. Cells* 82 (2004) 269.
22. Cullity B.D., Stock S.R., Elements of X-ray Diffraction (2001), Prentice-Hall, Pearson.
23. Gulino A., Fiorito G., Fragala I., *Mat. Chem.* 13 (2003) 861.
24. Maruyama T., Nakai T., *Sol. Energy Mat.* 23 (1991) 25.
25. Patil P.S., Kadam L.D., Lokhande C.D., *Thin Sol. Fil.* 272 (1996) 29.
26. Barreca D., Massignan C., Daolio S., Fabrizio M., Picirilllo C., Armelao L., Tondello E., *Chem. Mat.* 13 (2001) 588.
27. Mott N. F., Davis E. A., Electronic Process in Non-Crystalline Materials, second ed., Oxford University Press, London (1979).
28. Mott N. F., *Philos. Mag.* 19 (1969) 835

(2017) ; http://www.jmaterenvironsci.com/